Author Manuscript

Author Manuscript

Author Manuscript

Author Manuscript

HHS Public Access

Author manuscript

Bone. Author manuscript; available in PMC 2022 September 01.

Published in final edited form as:

Bone. 2022 September ; 162: 116471. doi:10.1016/j.bone.2022.116471.

Low bone mass and impaired fracture healing in mouse models of Trisomy21 (Down syndrome)

Kirby M. Sherman[a], **Diarra K. Williams**[a], **Casey A. Welsh**[a], **Alexis M. Cooper**[a], **Alyssa Falck**[a], **Shannon Huggins**[a], **Rihana S. Bokhari**[a], **Dana Gaddy**[b], **Kent D. McKelvey**[c,d], **Lindsay A. Dawson**[a], **Larry J. Suva**[a,*]

[a]Department of Veterinary Physiology and Pharmacology, College of Veterinary Medicine and Biomedical Sciences, Texas A&M University, College Station, TX 77843, United States of America

[b]Department of Veterinary Integrative Biosciences, College of Veterinary Medicine and Biomedical Sciences, Texas A&M University, College Station, TX 77843, United States of America

[c]Department of Family Medicine, University of Arkansas for Medical Sciences, Little Rock, AR 72205, United States of America

[d]Department of Medical Genetics, University of Arkansas for Medical Sciences, Little Rock, AR 72205, United States of America

Abstract

Individuals with Down syndrome (DS), the result of trisomy of human chromosome *Hsa21* (Ts21), present with an array of skeletal abnormalities typified by altered craniofacial features, short stature and low bone mineral density (BMD). While bone deficits progress with age in both sexes, low bone mass is more pronounced in DS men than women and osteopenia appears earlier. In the current study, the reproductive hormone status (FSH, LH, testosterone) of 17 DS patients (males, ages range 19–52 years) was measured. Although testosterone was consistently low, the hypothalamic-pituitary-gonadal axis was intact with corresponding rises in FSH and LH. To provide further insight into the heterogeneity of the bone mass in DS, the skeletal phenotypes of three of the most used murine DS models, Ts65Dn (Ts65), TC1, and Dp16(Yey1) (Dp16) were characterized and contrasted. Evaluation of the bone phenotype of both male and female 3-month-old Dp16 mice demonstrated sexual dimorphism, with low bone mass apparent in males, as it is in Ts65, but not in female Dp16. In contrast, male TC1 mice had no apparent bone phenotype. To determine whether low bone mass in DS impacted fracture healing, fractures of the middle phalanx (P2) digits were generated in both male and female Dp16 mice at 15 weeks of age, an age where the sexually dimorphic low BMD persisted. Fracture healing was assessed *via in vivo* microCT over (13 weeks) 93 days post fracture (DPF). At 93 DPF, 0 % of DS male (*n*

*Corresponding author at: Department of Veterinary Physiology and Pharmacology, College of Veterinary Medicine and Biomedical Sciences, Texas A&M University, College Station, TX 77843, United States of America. larry-suva@tamu.edu (L.J. Suva).

Supplementary data to this article can be found online at https://doi.org/10.1016/j.bone.2022.116471.

CRediT authorship contribution statement

DG, KDM, LAD, and LJS designed the research; KMS, DKW, CAW, AMC, AF, SH, LAD and RSB performed the research; KMS, DKW, CAW, AMC, AF, SH, DG, KDM, LAD and LJS analyzed the data; and KS, DG, LAD, and LJS wrote the manuscript.

Declaration of competing interest

The authors have declared that no conflict of interest exists.

Author Manuscript Author Manuscript Author Manuscript Author Manuscript

= 12) or female (n = 8) fractures healed, compared to 50 % of the male (n = 28) or female (n = 8) WT littermate fractures. MicroCT revealed periosteal unbridged mineralized callus formation across the fracture gap in Dp16 mice, which was confirmed by subsequent histology. These studies provide the first direct evidence of significantly impaired fracture healing in the setting of DS.

Keywords

Down syndrome; Fracture healing; Genetic mouse models; Osteopenia; Skeletal abnormalities

1. Introduction

Down Syndrome (DS), trisomy of human chromosome 21 (*Hsa21*) (Ts21), the most common birth defect in the United States, alters human development and leads to a variety of clinical issues such as mental impairment, heart defects, sleep apnea, hypogonadism, and infertility as well as growing reports of deficiencies in bone health [1–3]. However, unlike osteoporosis, the pathophysiology of many clinical aspects of the DS phenotype, such as low bone mass and the increased fracture rates, arise due to developmental deficits in bone mass accrual likely compounded by subsequent age-related bone loss. The past several decades has seen significant increases in the average life expectancy of individuals with DS, due in part to improved access to health care and the establishment of specialized health care guidelines [3–8]. Amidst the increase in longevity, skeletal complications such as osteopenia, bone fragility and fractures not previously recognized in the Ts21 community have begun to appear [9]. In addition, a recent meta-analysis demonstrated a significant association between BMD and Ts21. Individuals with Ts21 had a significantly decreased total and regional BMD when compared with the general population [10].

We have previously shown low BMD (corrected for bone size) and low bone turnover markers in 30 euthyroid healthy, calcium-replete, community dwelling people with Ts21 (17 male and 13 female, age range 19–52 years) compared with 26 non-DS controls (13 male and 13 female, age range 22–54 years) [11]. Our findings of low BMD and low bone turnover in people with Ts21 suggests that as they currently enjoy more active and independent lifestyles [3,4,12] they are now at an increased risk for falls and subsequent fracture, with limited treatment options. Indeed, as the life expectancy of individuals with Ts21 has increased to 60 in 2020 [3,4,8,13,14], the bone health of adolescent and adult Ts21 patients has become an important medical issue [7,15,16]. In situations of low bone turnover, anti-resorptive therapies such as bisphosphonates are not indicated, providing no viable treatment options for these at-risk patients [17]. Indeed, since Ts21 is considered a progeroid syndrome [18] adult individuals with Ts21 are known to present with clinical manifestations resembling elderly populations [1–3,19], including a particularly a high prevalence of osteoporosis, and as we and others have shown, decreased BMD [8,10,11].

Murine models of DS have been instrumental in elucidating the impact of Ts21 on development and homeostasis in mammalian species [20–23]. To dissect the mechanistic underpinnings of the varied Ts21 DS clinical phenotypes and to answer the question of how trisomy of Ts21 leads to the variable clinical presentation, animal models targeting

Author Manuscript Author Manuscript Author Manuscript Author Manuscript

single genes of chromosome 21 and the entire segments of genes have been developed. Genes found on *Hsa21* are spread over three mouse chromosomes *Mmu10*, *16* and *17* [21]. TC1 mice are transchromosomic for *Hsa21* generating a trans-species model of DS that contains ~83 % of the genes found on *Hsa21* and that exhibits phenotypic alterations in behavior, synaptic plasticity, cerebellar neuronal number, heart development, hypogonadism and mandible size consistent with DS [22]. In contrast, the Ts65Dn mouse strain is characterized by segmental trisomy for a region of *Mmu16* that contains approximately 75 % of *Hsa21*-homologous genes [24]. In Dp16(16)1Yey mice, 100 % of the entire *Hsa21* syntenic region of *Mmu16* is duplicated [7,25,26]. Ts65Dn, Dp16 and TC1 share the characteristic behavioral, reproductive, craniofacial, cardiac and myeloproliferative phenotype of people with DS [1,17] and all models are considered valid murine models of human DS phenotypes. Murine DS models (primarily Ts65Dn) have been shown to recapitulate skeletal abnormalities associated with DS, such as low BMD, early age-related bone loss, and sexual dimorphism and responsiveness to bone anabolic agents [27–30]. We hypothesized that the low bone turnover associated with DS would also compromise fracture healing. To investigate the impact of Ts21 on fracture repair, fractures were generated in the middle phalanx (P2) digits of both male and female Dp16 DS mice which surprisingly did not heal, even after 93 days. There is a need for an improved understanding of the DS bone phenotype and the apparent lack of appropriate fracture repair in the setting of DS. If recapitulated in humans, the impaired fracture healing response should be targeted with approaches that improve fracture healing and enhance bone mass.

2. Materials and methods

2.1. Human subjects

17 DS patients (males, ages range 19–52 years) attending the University of Arkansas Down syndrome clinic were recruited under a UAMS IRB approved protocol. All participants and/or their legal guardians gave informed consent prior to inclusion in the study. Each patient's clinical history was collected and a team of providers including MD, APN, dietician, occupational therapist evaluated the patient. Blood was drawn in the morning and endocrine hormones (FSH, testosterone and LH) measured in male DS patient serum at the same time in a single assay, using a single lot of reagents by a commercial clinical laboratory assay service (Mayo Clinic, Rochester, MN). Samples of venous blood were taken from all subjects into serum separator tubes. The blood was allowed to clot for 30 min at room temperature before centrifugation at 2500*g* for 10 min and storage at −20 °C. Preventive medicine care based on individual assessment and recommended labs for the assessment of male reproductive phenotype in people with DS were obtained [31].

2.2. Clinical bone mineral density (BMD)

Bone mineral density (BMD) of the PA spine and hip were assessed by dual-energy X-ray absorptiometry (DXA) using a Hologic Discovery A bone densitometer, located at the University of Arkansas for Medical Sciences. DXA equipment was calibrated with a lumbar spine phantom and step densities phantom following the Hologic guidelines. Measurements were obtained and analyzed using standard manufacturer's protocols. The World Health Organization (WHO) established criteria were used to classify bone health and osteoporosis

Author Manuscript Author Manuscript Author Manuscript Author Manuscript

[32]. Bone mineral density was measured at the spine, total hip, femoral neck, and distal radius as suggested by the International Society for Clinical densitometry (ISCD). The coefficient of variation of BMD was 1.7 % for femoral neck, 2.3 % for lumbar spine, 1.6 % for upper limbs and 0.9 % for lower limbs. The expression BMD/height (BMDH) was calculated to adjust bone mass for whole body bone size in DS patients as described [33].

2.3. Animal study design

All mice were maintained on a 12 h light/dark cycle, had *ad libitum* access to standard laboratory rodent chow and water, and were sacrificed by isofluorane anesthesia followed by cervical dislocation at the end of the experiment. All animal experiments were initiated with mice at peak adult bone mass (minimum of 3 months of age for all DS strains examined). Only male trisomic B6EiC3Sn *a/A*-Ts(17^{16})65Dn/J (Ts65Dn) mice and wild-type (WT: B6EiC3Sn.BLiAF1/J) mice were analyzed due to the sub-fertile nature of male mice and the lack of commercial availability of female mice at the time of the study, due to the importance of female mice in colony maintenance (Jackson Laboratory, Bar Harbor, ME). Ts65Dn mice are trisomic for 152 genes on mouse chromosome 16 (*Mmu16*) [24].

TC1 (Tc(HSA21)1TybEmcf) mice (Jackson Laboratory) are viable, fertile, and normal in size, and only the female carriers consistently transmits the mutation to the germline. TC1 mice contain 42 Mb (approximately 83 %) of freely segregating *Hsa21* containing 158 of 213 functionally trisomic protein coding genes including most of the gene orthologs located on *Mmu10*, *Mmu16*, and *Mmu17*, which have been found to contribute to DS [22]. TC1 mice were until recently the only transchromosomic DS mouse model [34]. *Hsa21* in TC1 has over 50 protein-coding genes disrupted. As with Ts65Dn, only male TC1 mice were commercially available at time of analysis. The appropriate WT control for male TC1 was littermates from the colony of the B6129S8F1/J strain (Jackson Laboratory).

Both male and female Dp16(1)Yey mice were commercially available (Jackson Laboratory) and analyzed in this study. These mice contain a duplication orthologous to human 21q11-q22.3 and carry 113 genes orthologous to genes on *Hsa21* [25]. We were able to study both male and female DS mice only in the context of the Dp16 strain. The appropriate WT control for male and female Dp16 were littermates from the colony of the C57BL/6J;129S7/SvEvBrd strain (Jackson Laboratory). All animal procedures were approved by and performed in accordance with the guidelines of the Texas A&M University IACUC. All male DS and WT lines were housed individually. All DS lines and WT controls purchased from the Jackson Laboratory had genotype confirmed upon arrival at Texas A&M University using established and published protocols [2,7,30].

2.4. Bone mineral density (BMD)

Dual-energy X-ray absorptiometry (UltraFocus DXA, Faxitron, Tucson, Arizona) was used to measure total body (excluding the head region), hindlimb and spine BMD (g/cm^2) as we have previously described [28,35]. Measurements were acquired at baseline and at the end of the study. Sub-region analysis of the mid-shaft of the tibia and femurs of all mice was also performed [35]. The precision of DXA in our laboratory is 1.7 % [30].

Author Manuscript Author Manuscript Author Manuscript Author Manuscript

2.5. Analysis of trabecular and cortical bone by micro computed tomography (microCT)

Formalin-fixed tibiae were imaged using high-resolution micro-computed tomography (μCT50, Scanco Medical, Brüttisellen, Switzerland). Briefly, the proximal tibia and tibial midshaft regions were scanned as 9 μm isotropic voxel size using 55 kVp, 114 mA, and 200-ms. Bone volume fraction (BV/TV, %), trabecular thickness (Tb.Th, mm), trabecular separation (Tb.Sp, mm), trabecular number (Tb.N, 1/mm), connectivity density (ConnD 1/mm^3), and structure model index (SMI) were calculated using previously published methods [36]. The cancellous bone region was obtained using a semi-automated contouring program that separated cancellous from cortical bone. At the midshaft of the tibia, total cross sectional area (CSA, mm^2), medullary area (MA, mm^2) and cortical thickness (Ct.Th, mm) were assessed in a 1 mm long region centered at the midshaft. Bone was segmented from soft tissue using the same threshold for all groups, 245 mg HA/cm3 for trabecular and 682 mg HA/cm^3 for cortical bone. All microCT scanning and analyses were compliant with American Society for Bone and Mineral Research (ASBMR) guidelines for rodents [37].

2.6. Histology and bone histomorphometry

Quantitative dynamic histomorphometry was performed on paraffin and methyl methacrylate-embedded tibiae as we have previously described [35,36,38]. Calcein (15 mg/kg) and alizarin red complexome (40 mg/kg) were injected intraperitoneally 7 and 2 days, respectively, prior to sacrifice. Histomorphometric measurements were performed on the secondary spongiosa of the proximal tibia metaphysis using OsteoMeasure (SciMeasure, Decatur, GA). For dynamic histomorphometry, mineralizing surface per bone surface (MS/BS, %) and mineral apposition rate (MAR, μm/d) were measured in unstained sections under ultraviolet light and used to calculate bone formation rate with surface referent (BFR/BS, $\mu m^3/\mu m^2$/d) [35,36]. Terminology and units adhere to the recommendations of the ASBMR histomorphometry nomenclature committee [39]. Fractured P2 digits were fixed, decalcified, paraffin processed, and sectioned as we have previously described [40].

2.7. Ex vivo bone marrow cultures

Bone marrow cells were harvested from femurs of 3–4 month old mice (Dp16 and Ts65Dn) and cultured as previously described [41]. In brief, for osteoclastogenesis cells were flushed from femurs, washed, and cultured in 24-well plates (Becton Dickinson Labware) at a density of 2×10^6 cells per well in α-minimal essential medium (α-MEM), supplemented with 15 % fetal calf serum, and 10^{-8} M 1,25-dihydroxyvitamin D3 ($1,25(OH)_2D_3$) in quadruplicate wells per treatment. Cells were fed every 3 days with half-volumes of medium, until day 10, when cells were fixed and stained with tartrate resistant acid phosphatase (TRAP) to facilitate determination of the number of TRAP-positive multinucleated (3 or more nuclei) cells formed per well. For osteoblastogenesis, bone marrow cells harvested from femurs were seeded in triplicate at 1×10^6 cells/well in 12-well tissue culture plates (Becton Dickinson Labware) containing osteoblast medium (α-MEM +15% FBS containing 10 mM BGP and 50 μM ascorbic acid). The recruitment of mesenchymal progenitors into the osteoblastic lineage was determined by alkaline phosphatase-positive (AP+) staining for colony forming unit-fibroblast (CFU-F) on day 10 and differentiation measured by alizarin red staining of mineralized cultures on day 28

Author Manuscript Author Manuscript Author Manuscript Author Manuscript

(CFU-OB). The number of AP+ colonies and total colonies were enumerated as described [41].

2.8. P2 fracture studies

The P2 bone is the middle phalanx in the digit and is located central to the dorsal elastic claw ligament and the ventral deep digital tendon. P2 fractures are performed bilaterally on hind limb digits 2 and 4, thus utilizing 4 digits total from each animal to create 4 independent fractures. Akin to other musculoskeletal studies using the digit as a model system, this increases reproducibility and maximizes fractures while minimizing animal use [42–45]. Digit 3 serves as an uninjured control. The P2 fracture plane uses the second ventral digital fat pad indent as a visual landmark to ensure fracture consistency. P2 open fractures are created using micro-scissors to create a fine incision to expose the P2 bone, followed by fracturing the bone and severing the dorsal elastic claw ligament using small surgical scissors. The dorsal elastic claw ligament is a taut structure that traverses the length of the P2 bone, linking the proximal region of the P2 bone to the dorsal base of the terminal phalanx (P3) bone, and is severed to allow proper alignment of the P2 fracture fragments [45]. The incision is closed using the skin adhesive, Dermabond™. Due to the small size of the fractured P2 bone, further fixation and stabilization was not necessary [45]. Sequential *in vivo* microCT of all digits in the same mouse over the course of fracture healing was performed from 0 days post-fracture (DPF) to 93 DPF.

2.9. Statistical analysis

Based on our previous examinations of bone mass and volume in Ts65Dn DS mice [28,30,46], a power analysis prior to the start of this study suggested $n = 5–8$ per group would provide sufficient power (0.8) to detect a significant difference for all endpoints between WT and the corresponding DS mouse lines. All data points were checked for normality, and standard descriptive statistics computed. Comparisons within genotype (*e.g.* WT or Ts65Dn; WT or TC1; WT or Dp16) were performed using Student's *t*-test as appropriate using Prism 5 (GraphPad Software, San Diego, CA, USA). Data are presented as mean ± S.D. and differences were considered significant at $p < 0.05$ and are reported as such. Data graphs display all individual data points to show the distribution of the data. Serum measurements were collected and plotted for each patient individually. No comparisons were made for any DS patients hormone levels and serum values only are reported.

3. Results

3.1. Low testosterone and functional hypothalamic-pituitary-gonadal (HPG) axis in men with DS

We have previously reported low bone turnover markers and bone mineral density (BMD) in a cohort of people with Ts21 without consistent clinical risk factors [11]. In this cohort, 7 of 13 (54 %) Ts21 DS females and 12 of 17 (71 %) Ts21 DS males had low bone mass at one of the measured sites ($Z \leq -2.0$) [11]. Subsequently, a more detailed examination of the BMD and reproductive hormone profiles of the 17 DS males was undertaken. The distribution of Z scores 0 to −1.5; −1.5 to −2.5, and < −2.5 for BMD measured at the

Author Manuscript Author Manuscript Author Manuscript Author Manuscript

femoral neck revealed that 50 % of males with DS had Z scores less than −1.5, with 5 % being in the osteoporotic range (Z ≤ −2.5) (Fig. 1A). At the posterior-anterior (PA) spine, only 24 % had Z scores in the 0 to −1.5 range, with the remaining individuals −1.5, and 13 % in the osteoporotic range (Z ≤ −2.5) (Fig. 1A). Given the distribution of BMD Z scores and in the face of the low bone turnover marker levels in this patient cohort [11], hormones in the hypothalamic-pituitary-gonadal (HPG) axis were measured.

Serum testosterone, luteinizing hormone (LH) and follicle stimulating hormone (FSH) were measured. As expected for cohorts of males with DS, serum testosterone was low, at the lower limit of the normal range (2.5–11 ng/mL) (shaded area, Fig. 1B) although the mechanism responsible for the documented low serum testosterone and subfertility or infertility in DS men remains unknown [47]. The consistently low serum testosterone in the cohort resulted in corresponding elevations in LH (Fig. 1C) and FSH (Fig. 1D) that in some individuals was well beyond the normal range (LH 1.2–7.1 mIU/mL; FSH 2–8.3 mIU/mL), indicating that hypothalamic and pituitary responses to low testosterone remain intact and that disruption of the HPG axis does not account for low testosterone. These data provided the rationale to investigate whether the same heterogeneity in BMD and bone accrual persisted across multiple strains of DS mice.

3.2. Examination of the skeletal phenotype of murine DS models

We and others have previously demonstrated [27,28,30,46,48] low BMD and bone accrual in Ts65Dn DS mice, and recently the skeletal phenotype of a related Dp16 DS mouse line (Dp1Tyb) was reported [49]. However, a direct comparison of bone phenotypes across multiple lines including the Dp16(1)Yey (Dp16) as a model for the distribution of bone mass in Ts21 patients has not been reported. Therefore, the bone phenotype of the most widely available and well-established DS mouse models (Ts65Dn; TC1; Dp16) (Fig. 2A–C) was determined. The Ts65Dn bone phenotype has been previously reported [28] and is included herein as confirmation of the bone phenotype at 3 months of age. As shown (Fig. 2A, B) 3 month-old male Ts65 and Dp16 mice have significantly lower BV/TV compared to the appropriate WT control. Interestingly, the BV/TV of female Dp16 (Fig. 2B) and male TC1 mice (3 months of age) (Fig. 2C) do not significantly differ from the BV/TV of their respective WT (and gender) controls. These analyses suggest that just as in Ts21 humans, there is a heterogeneity in the low bone mass phenotype across various DS mouse lines that replicates the tendency for low bone mass in males *versus* females [7,11]. Given the lack of any discernable bone phenotype in 3 month old male TC1 mice, we also measured bone accrual in TC1 mice out to 6 months, to ensure that the lack of bone phenotype at three months was not aberrant (Supplemental Fig. 1). No significant difference in BMD (or BV/TV) was observed at any age in both WT (B6129S8F1/J) and TC1 mice littermates (Supplemental Fig. 1 $n = 5$ per group). Next, the measurement of bone formation rate (BFR) in all three lines of DS male mice (and appropriate WT controls) demonstrated that both male Ts65Dn and Dp16 mice had significantly decreased BFR compared with WT, whereas the BFR in TC1 male mice was not different from WT littermates (Fig. 2D–F).

Next, body weight over time (Supplemental Fig. 2) and the trabecular and cortical bone phenotype of male and female Dp16 mice and the appropriate WT littermate

Author Manuscript Author Manuscript Author Manuscript Author Manuscript

controls (C57BL/6J;129S7/SvEvBrd) was determined (Supplemental Fig. 3) using microCT. Trabecular architecture and cortical geometry analyses (Supplemental Fig. 3) confirmed the dimorphic trabecular bone phenotype, with significant decreases in trabecular number (Tb.N.) explaining the male-specific decrease in trabecular bone volume. Regarding cortical bone geometry, male Dp16 mice had significantly decreased cortical bone, with no change in cortical thickness, presumably related to the age (12 weeks) at the time of phenotyping. With increased age, a difference will presumably become apparent consistent with decreased medullary/cross sectional area and endosteal/periosteal perimeter (Supplemental Fig. 3). The other cortical parameters, medullary area, periosteal perimeter, endosteal perimeter, and total cross-sectional area were all significantly decreased in male Dp16 mice (Supplemental Fig. 3). No differences in any trabecular or cortical bone parameters were observed in female Dp16 mice.

To gain insight into the cellular mechanism(s) for the differences in bone phenotype between male and female Dp16 mice, *ex vivo* bone marrow cultures were performed. In these studies, bone marrow derived precursors were differentiated towards either the osteoblast or osteoclast lineages (Fig. 3) as previously described [28,30]. Interestingly, although no differences in trabecular and cortical bone architecture and geometry were observed in female Dp16 mice, significant increases in osteoblast recruitment (Fig. 3A) and the total number of mesenchymal progenitors (Fig. 3B) were observed in both male and female Dp16 mice. The capacity for osteoblast mineralization *in vitro* (Fig. 3C) was also significantly increased in female Dp16. On the osteoclastogenic side, only male Dp16 mice had significantly increased osteoclastogenesis, with no significant decrease observed in female Dp16 mice (Fig. 3D), that have no discernible change in bone volume (Fig. 2B). Collectively, the low bone mass of male Dp16 mice is the result of elevated bone resorption, which overcomes the elevated ability to recruit cells into the osteoblast lineage but fail to develop into functional osteoblasts. This is a significant departure from male Ts65Dn mice in which low osteoblast and osteoclast formation is responsible for the low bone mass (Supplemental Fig. 4) [27,28].

3.3. Fracture healing is impaired in Dp16 DS mice

To investigate bone healing in Dp16 mice, the P2 fracture healing response in male and female Dp16 DS mice and male and female WT littermate controls was monitored weekly from 0 days post-fracture (uninjured), up to 93 DPF using *in vivo* microCT imaging (Fig. 4). Both male and female Dp16 and WT controls had a similar weight gain across the entire experimental time course (Supplemental Fig. 2). Reconstructed microCT images for a single P2 digit across the timeline of fracture healing for male (Fig. 4B) and female (Fig. 4C) WT mice from 0 DPF to 93 DPF show a normal spectrum and progression of fracture healing in WT mice, including periosteal hard callus formation, bony bridging, and remodeling evident by 93 DPF. In the male Dp16 DS digit, while a hard callus is forming at 21 DPF, it is not sufficient to result in a bridged fracture by 42 DPF (Fig. 4B) leading to non-union at 93 DPF. If the fractures did not initiate bridging by 42 DPF, bridging was not observed. Of the 12 male digits analyzed, no fractures healed in Dp16 male mice compared to 50 % in their WT male littermates ($n = 28$ digits). Similarly, no fractures healed in female Dp16 mice ($n = 8$) compared to 50 % of the WT littermate female fractures ($n = 16$ digits) (Fig. 4C). In Dp16

Author Manuscript Author Manuscript Author Manuscript Author Manuscript

females, all 8 digits were non-unions compared to the WT females which each had 2 digits heal of the 4 fractured.

To quantitatively assess fractures, we developed a fracture scoring method, the Computed Radiographic Assessment of P2, or CRAPP (Fig. 5). This method using *in vivo* microCT was adapted from the radiographic union score for tibial fractures (RUST) scoring system developed for tibial fracture healing after intramedullary fixation in humans by Whelan et al. [50], which is currently considered the gold standard for fracture scoring using 2D radiographs [51]. In our assessment, a CRAPP fracture score of I is defined as a non-union with the fracture line visible and no bridging observed within the fracture gap (Fig. 5A). A score of II has a visible fracture line but shows <50 % bridging within the fracture gap. A score of III contains a visible fracture line with >50 % bridging in the fracture gap. Finally, a score of IV is defined as a complete union with no apparent fracture line and the fracture gap has been completely bridged with hard, bony callus (Fig. 5A). The CRAPP method was then used to quantify P2 fracture healing in WT and Dp16 male and female mice using the scale from I-IV: I a non-union fracture and IV a union (Fig. 5A). It is important to note that in bones scoring between scores, the lower score was assigned. The analysis revealed that in Dp16 mice, fracture repair is significantly impaired with no Dp16 fractures scoring above II (<50 % bridging) using the CRAPP method (Fig. 5B). 13 of 28 fractures (46 %) in male WT mice received a CRAPP score of I (non-union) compared to 11 of 12 (92 %) male Dp16 fractures (Fig. 5B). Similarly, 7 of 16 (44 %) female WT fractures scored I compared to 8 of 8 (100 %) of female Dp16 fractures scoring I (Fig. 5B). Overall, a range of normal fracture healing was observed in WT males and females that was not observed in Dp16 mice of either sex. Indeed, the normal range of fracture healing observed in WT animals provides evidence that P2 fractures performed on the same animal are in fact independent of each other. Histologically, Safranin-O Fast Green staining revealed that fracture healing was evident in WT male mice (93DPF), with no fracture plane visible and woven bone remodeled to cortical bone (Fig. 6A). In the <50 % WT fractures that did not heal, histological evaluation revealed marked cartilaginous matrix staining by Safranin O (Fig. 6A). However, healing was absent in male Dp16 (93DPF) (Fig. 6A) without any evidence of the unmineralized cartilage matrix in the fracture gap that was observed in WT non-unions. Similar histological results were observed in female WT and Dp16 DS mice (Fig. 6B). Together, the data confirms the microCT observations that both male and female Dp16 DS mice fail to heal P2 fractures, but also indicate that DS non-union healing is mechanistically distinct from WT non-unions.

4. Discussion

There is no perfect animal model for a human disease [52], and perhaps even less so for a complex genetic disorder such as DS [34]. DS mouse models have been invaluable tools for advancing knowledge of the underlying mechanisms driving physiologic and behavioral abnormalities in people with DS. In the complex environment of DS, as with all animal models, investigators seek a model that reflects the human phenotype of interest, such as abnormalities in heart and brain development, learning deficits, or in our case low bone mass and impaired fracture healing. However, deciphering causality in these (and all other) murine DS models has proven to be very complex given the distribution and genetic

Author Manuscript Author Manuscript Author Manuscript Author Manuscript

make-up of mouse *Hsa21* orthologous genes [2]. In doing so, significant research effort has focused on the examination of individual DS murine models and normalizing expression of trisomic genes in DS to correct aspects of the Ts21 phenotype, but with limited success [7,53,54]. We have been continuously studying the Ts65Dn mouse model for over 10 years and routinely repeat previously published measures of low bone accrual and BMD to ensure the presence of bone phenotype across cohorts of Ts65Dn animals. Certainly, difficulties associated with breeding, and inconsistent phenotypes in Ts65Dn mice highlight specific caveats with the use of this model [54]. In addition, the strictly controlled accessibility to DS mice strains, that is finally relaxing, has contributed to the extensive singular focus primarily on the Ts65Dn strain. This focus has broadened recently with the wider availability of additional trisomic models such as Dp16 and Dp1Tyb [7,49]. However, we hypothesized that the strategy (focusing on single genes and any single animal model) has major limitations and drove our efforts to pursue a broad multi-strain approach similar to that employed in studies utilizing the Collaborative Cross mouse populations [55–57].

In this setting, the assessment of the skeletal phenotype and other skeletal responses such as fracture healing or bone regeneration across several DS murine models (Ts65Dn, TC1, Dp16) offers meaningful insight into the complex regulatory pathways regulating bone mass in DS. Skeletal analysis across these DS strains provides the best current opportunity to support preclinical studies aimed at ameliorating the osteopenia of Ts21 and maximizing bone mass and strength in people with DS. This strategy should define the heterogeneity of the low bone mass phenotype that we and others have observed in DS mouse models [27,28,30,48] and better model the heterogeneity of bone mass observed in Ts21 humans [11,58–61]. Our skeletal phenotyping analyses revealed that male DS Ts65Dn and Dp16 mice have lower BMD and bone turnover than WT counterparts, whereas male TC1 lack any discernible bone phenotype. As we had observed in DS females with Ts21 who exhibit low BMD less frequently than males [11,61,62], female Dp16 mice do not present with the low bone mass phenotype of age-matched male Dp16 mice at any age we have examined. The significant osteopenia in male Dp16 DS mice was the result of decreased bone accrual and increased osteoclastogenesis. The differences in cellular mechanism underlying the low bone mass bone phenotypes of Ts65Dn and Dp16 mice may also explain the sex-specific differences in bone mass observed in male and female Dp16 DS mice. This is different from studies of bone mass in Dp1Tyb mice that revealed significant differences in trabecular and cortical bone between male and female DS mice and euploid littermates at 6 and 16 weeks of age [49]. We interpret this difference as further evidence supporting the value of examining multiple lines of DS mice and presumably associated with the genetic differences between Dp16 and Dp1Tyb mice. In addition, it is well recognized that the background on which a trisomic animal is bred influences the phenotypic characterization of the animals [63] suggesting that the complex genetic landscape of trisomic mice maybe more susceptible to allelic differences in background strains that affect phenotypes [54]. However, it is important to recall that in Ts21 humans, there is a sexual dimorphism, and females with low BMD are less frequent than males [10,54,55].

Histomorphometric analysis of the secondary spongiosa of the proximal tibia of 5-month old Ts65Dn and Dp16 male mice confirmed the low BMD phenotype and demonstrated it was associated with decreased bone formation rate (BFR) per bone surface. TC1 DS mice

Author Manuscript Author Manuscript Author Manuscript Author Manuscript

had no bone phenotype or demonstrable decreases in bone formation (Fig. 2). In addition, we have demonstrated previously that the low bone mass in Ts65Dn mice is the result of low bone turnover and that the low BMD can be ameliorated by treatment with intermittent PTH therapy [28], or weekly SclAb treatment [30,46]. Thus, the distinct skeletal phenotypes of three DS models highlight the differences in architectural parameters as well as cellular mechanism(s) in play across the Ts21 spectrum.

Ex vivo bone marrow cultures from Ts65Dn, Dp16 and WT littermates were cultured towards osteoclasts and osteoblasts, identifying a distinct mechanism driving low bone mass in male Ts65Dn (low bone accrual/low bone turnover) compared with male Dp16 (increased bone resorption/low bone formation). The situation in female Dp16 (no difference in bone mass compared with WT control females) shows an interesting parallel with humans, where low bone mass appears more prevalent in males with DS than females [7,11]. These cellular findings differ from the consistently suppressed osteoblast and osteoclast differentiation we and others have reported in male Ts65Dn [27,28] and Dp1Tyb [49] that provides the cellular basis for the low bone mass found in these mouse models of DS. In addition, the lack of any observed bone volume changes in female Dp16 mice is presumably the result of an increased capacity of osteoblast recruitment and increased ratio of osteoblast maturation without altering osteoclastogenesis. The spectrum of skeletal phenotypes presented by Ts65Dn, Dp16 and TC1 DS mice provides compelling evidence to support our contention that the examination of multiple DS mouse lines informs the heterogeneity of Ts21 in humans.

Several factors have contributed to the utility of mouse models to study fracture repair, including low cost, genetically modified strain availability, rapid fracture healing time, and the development of specific fixation systems capable of repairing small murine bones. In particular, the ideal fracture model would be inexpensive, reproducible, not encumbered with technical difficulties, and have the potential for high throughput [64]. To investigate fracture healing in DS mice, we utilized a novel P2 fracture model of the adult mouse digit that fulfills these particular criteria, but that does not require external or internal fixation post-fracture as required in tibia and femur fracture healing models [45]. As in femur and tibia fractures, P2 fracture initiates the phases of inflammation, cartilaginous callus formation, woven callus formation, and secondary bone remodeling [45]. In this model, animals are fully mobile and able to ambulate normally post-surgery. However, unlike tibia and femur fracture models in which significant numbers of fractures may need to be excluded if the induced fractures are misaligned, have an irreparable break, lose fixation during healing, acquire fracture site infections or other processing artifacts [65], no such exclusions occur with P2 fractures. Indeed, following P2 fracture the mice freely ambulate, appear to be in no discomfort and eat and behave normally. As shown, Dp16 male and female body weights are not different from WT controls and all continue to gain weight up to 28 weeks of age (Supplemental Fig. 2). In this study, a range of fracture healing responses was observed in both WT and Dp16 mice, providing insight into the biology of fracture repair unencumbered by experimental variation or post-fracture surgery exclusion.

We hypothesized that fracture healing in Dp16 DS mice would be delayed, so the complete lack of fracture healing in male and female Dp16 P2 fractures was entirely unexpected.

Author Manuscript Author Manuscript Author Manuscript Author Manuscript

Further examination identified no evidence of callus bridging across the time course of fracture healing, even out to 93DPF in either sex, at which time WT fractures were healed and actively undergoing bone remodeling. Interestingly, the sexually dimorphic low BMD between male and female Dp16 was maintained even in animals 93 DPF, at which time animals were approximately 6–8 months of age.

In WT mice, the periosteal cartilaginous callus bridges the P2 fracture gap, followed by hard callus bridging [45]. The low number of unbridged WT nonunion fractures exhibited marked cartilage matrix in the fracture gap that incompletely converted to hard callus bridging. However, in Dp16 fractures, the hard callus was observed along the surface of the fracture fragments but not within the fracture gap, and in the absence of any cartilaginous matrix in the fracture gap. These data provide compelling evidence to suggest that the early phases of fracture repair, possibly including cartilage formation and subsequent mineralization, are aberrant in male and female Dp16 mice. Ongoing studies are focused on identifying the DS-related deficits in chondrocyte differentiation, cartilage formation and mineralization that impair fracture healing.

Traditionally, 2D X-rays have been utilized to display the progression of fracture healing, with minimal attempts to generate quantitative data [51]. The radiographic union score for tibial fractures (RUST) [50] as well as modified RUST (mRUST) [66], an adjusted RUST score, rely on plain, 2D X-rays. Both scoring methods have been validated in human tibial fractures and evidence supporting utility of RUST and mRUST in murine fracture studies is available [67]. RUST and mRUST have an excellent relationship to both structural and biomechanical parameters and are positively correlated with BMD, bone volume/tissue volume (BV/TV), callus strength, and callus rigidity [67]. However, advances in imaging in rodents, namely *in vivo* microCT afforded us the opportunity to better assess the extent of fracture healing *in vivo* in 3 dimensions and with 360° image analysis capabilities. To better assess the DS fractures in our P2 fracture model, a system utilizing *in vivo* microCT termed Computed Radiographic Assessment of P2 (CRAPP) was developed. Using CRAPP, no male or female DS fractures show any evidence of bone repair or healing, compared to 50 % of fractures that were fully healed in WT male and female littermates. The lack of healing observed *via* microCT was confirmed histologically at timepoints out to 93DPF, which show a significant difference in how DS fractures heal compared to their WT littermates. Ongoing studies are examining the lack of P2 fracture healing in DS and investigating the apparent attenuated formation of the cartilaginous callus during P2 fracture repair in the setting of DS. These data introduce a new microCT-based quantitative approach to fracture repair assessment and provide the first direct evidence of impaired fracture healing in DS. If validated in human Ts21 patients, these studies suggest Ts21 fractures are at risk of delayed healing, with the associated morbidity and mortality consequences.

While the life expectancy of people with DS has increased [3,8], so has the incidence of fractures due to a low bone mineral density, which negatively impacts quality of life for DS patients. Although the most common fractures involve small bones of the hands and feet, elderly patients are more likely to fracture major bones from a fall than younger patients [68]. Interestingly, a health care review of 38 Ts21 adults revealed that Ts21 individuals showed a high incidence of osteoporosis with resultant fractures of both the long bones and

Author Manuscript Author Manuscript Author Manuscript Author Manuscript

vertebral bodies [69]. These data have been reinforced by a meta-analysis that demonstrated decreased total and regional BMD in Ts21 individuals when compared with the general population [10] and as we had described previously in our cohort of Ts21 patients [11].

Given the typical hypogonadal phenotype observed in DS male patients [1,3,11], it was expected that people with Ts21 would exhibit high bone turnover. However, our report of low bone turnover markers in Ts21 patients [11] suggests bone turnover markers may be independent of hypogonadism. In the 17 men with Ts21, the mean serum levels of FSH and LH were elevated, in some cases above the normal range for men. By contrast, the mean plasma level of testosterone for all Ts21 men (except 1) were in the low-normal range, reflecting a diagnosis of low-normal gonadal function and an intact hypothalamic-pituitary-gonadal axis capable of responding to the low-normal testosterone levels. Currently, future studies are needed to uncover the cause of the inherent low bone turnover in DS men in the face of low testosterone. We are approaching this in the multiple mouse models of DS and are actively interrogating the endocrine markers in all of the DS mice lines we are currently investigating.

The studies described herein provide the first evidence that bone healing is impaired in the setting of DS and provides a strong rationale to explore treatment options that enhance fracture healing in DS mice and that may be translated to Ts21 patients. In other studies, we have attempted to utilize medical databases for details of DS patient fractures to no avail. It is an important next step to determine the extent to which Ts21 humans are affected by diminished fracture healing. Our ongoing studies are seeking to: 1) determine how the different DS mouse models respond to fractures as well as other models of bone healing, 2) further investigate how Ts21 impacts bone health, and 3) understand the pathophysiology behind the low bone mass phenotype and aberrant bone healing and cartilage deficits in DS mice. These findings suggest that increased, active interventions must be implemented to effectively control low bone mass issues, and importantly, treat osteoporosis and minimize fracture risk in individuals with Ts21 [8].

Supplementary Material

Refer to Web version on PubMed Central for supplementary material.

Acknowledgements

Our investigation of trisomy Hsa21 (Down syndrome) is dedicated to our co-author, friend, and close colleague Dr. Kent D. McKelvey. As a clinical geneticist, Kent’s love and caring for the families and people with Down syndrome remains our daily inspiration. Kent’s knowledge and enthusiasm are sorely missed. These studies were supported by 1R01HD102909 (to LJS), R21-DE028076, T35-OD010991 (to DG for support of CAW), an APS Porter Fellowship (to DKW) and by the College of Veterinary Medicine & Biomedical Sciences at Texas A&M University. The content is solely the responsibility of the authors and does not necessarily represent the official views of the National Institutes of Health. The funders were not involved in study-design, data collection, data analysis, manuscript preparation and/or publication decisions.

The data that support the findings of this study and Down syndrome mouse models are available from the corresponding author upon reasonable request.

Author Manuscript Author Manuscript Author Manuscript Author Manuscript

References

[1]. Hawli Y, Nasrallah M, El-hajj fuleihan G, endocrine and musculoskeletal abnormalities in patients with down syndrome, Nat. Rev 5 (6) (2009) 327–334.

[2]. LaCombe JM, Roper RJ, Skeletal dynamics of down syndrome: a developing perspective, Bone 133 (2020), 115215. [PubMed: 31887437]

[3]. Bull MJ, Down syndrome N. Engl. J. Med 382 (24) (2020) 2344–2352. [PubMed: 32521135]

[4]. Glasson EJ, Sullivan SG, Hussain R, Petterson BA, Montgomery PD, Bittles AH, The changing survival profile of people with Down's syndrome: implications for genetic counselling, Clin. Genet 62 (5) (2002) 390–393. [PubMed: 12431254]

[5]. Coppus AM, Evenhuis HM, Verberne GJ, Visser FE, Oostra BA, Eikelenboom P, van Gool WA, Janssens AC, van Duijn CM, Survival in elderly persons with down syndrome, J. Am. Geriatr. Soc 56 (12) (2008) 2311–2316. [PubMed: 19093931]

[6]. Bosch JJ, Health maintenance throughout the life span for individuals with down syndrome, J. Am. Acad. Nurse Pract 15 (1) (2003) 5–17. [PubMed: 12613408]

[7]. Thomas JR, Roper RJ, Current analysis of skeletal phenotypes in down syndrome, Curr. Osteoporos. Rep 19 (3) (2021) 338–346. [PubMed: 33830429]

[8]. Tsou AY, Bulova P, Capone G, Chicoine B, Gelaro B, Harville TO, Martin BA, McGuire DE, McKelvey KD, Peterson M, Tyler C, Wells M, Whitten MS, W., Global down Syndrome Foundation medical care guidelines for adults with down syndrome, medical care of adults with Down syndrome: a clinical guideline, JAMA 324 (15) (2020) 1543–1556. [PubMed: 33079159]

[9]. Yang Q, Rasmussen SA, Friedman JM, Mortality associated with Down's syndrome in the USA from 1983 to 1997: a population-based study, Lancet 359 (9311) (2002) 1019–1025. [PubMed: 11937181]

[10]. Zhang Y, Tian Z, Ye S, Mu Q, Wang X, Ren S, Hou X, Yu W, Guo J, Changes in bone mineral density in down syndrome individuals: a systematic review and meta-analysis, Osteoporos. Int 33 (1) (2022) 27–37.

[11]. McKelvey KD, Fowler TW, Akel NS, Kelsay JA, Gaddy D, Wenger GR, Suva LJ, Low bone turnover and low bone density in a cohort of adults with down syndrome, Osteoporos. Int 24 (4) (2013) 1333–1338. [PubMed: 22903293]

[12]. Bittles AH, Glasson EJ, Clinical, social, and ethical implications of changing life expectancy in down syndrome, Dev. Med. Child Neurol 46 (4) (2004) 282–286. [PubMed: 15077706]

[13]. Zigman WB, Atypical aging in down syndrome, Dev. Disabil. Res. Rev 18 (1) (2013) 51–67. [PubMed: 23949829]

[14]. Presson AP, Partyka G, Jensen KM, Devine OJ, Rasmussen SA, McCabe LL, McCabe ER, Current estimate of down syndrome population prevalence in the United States, J. Pediatr 163 (4) (2013) 1163–1168. [PubMed: 23885965]

[15]. Lohiya GS, Crinella FM, Tan-Figueroa L, Caires S, Lohiya S, Fracture epidemiology and control in a developmental center, West J. Med 170 (4) (1999) 203–209. [PubMed: 10344173]

[16]. Schrager S, Kloss C, Ju AW, Prevalence of fractures in women with intellectual disabilities: a chart review, J. Intellect. Disabil. Res 51 (Pt 4) (2007) 253–259. [PubMed: 17326806]

[17]. Kamalakar A, Harris JR, McKelvey KD, Suva LJ, Aneuploidy and skeletal health, Curr. Osteoporos. Rep 12 (3) (2014) 376–382. [PubMed: 24980541]

[18]. Martin GM, Genetic syndromes in man with potential relevance to the pathobiology of aging, Birth Defects Orig. Artic Ser 14 (1) (1978) 5–39.

[19]. Vetrano DL, Carfi A, Brandi V, L'Angiocola PD, Di Tella S, Cipriani MC, Antocicco M, Zuccala G, Palmieri V, Silveri MC, Bernabei R, Onder G, Left ventricle diastolic function and cognitive performance in adults with Down syndrome, Int. J. Cardiol 203 (2016) 816–818. [PubMed: 26595792]

[20]. Olson LE, Richtsmeier JT, Leszl J, Reeves RH, A chromosome 21 critical region does not cause specific Down syndrome phenotypes, Science (New York, N.Y.) 306 (5696) (2004) 687–690.

Author Manuscript Author Manuscript Author Manuscript Author Manuscript

[21]. Antonarakis SE, Lyle R, Dermitzakis ET, Reymond A, Deutsch S, Chromosome 21 and down syndrome: from genomics to pathophysiology, Nat. Rev. Genet 5 (10) (2004) 725–738. [PubMed: 15510164]

[22]. O'Doherty A, Ruf S, Mulligan C, Hildreth V, Errington ML, Cooke S, Sesay A, Modino S, Vanes L, Hernandez D, Linehan JM, Sharpe PT, Brandner S, Bliss TV, Henderson DJ, Nizetic D, Tybulewicz VL, Fisher EM, An aneuploid mouse strain carrying human chromosome 21 with Down syndrome phenotypes, Science (New York, N.Y.) 309 (5743) (2005) 2033–2037.

[23]. Levenga J, Peterson DJ, Cain P, Hoeffer CA, Sleep behavior and EEG oscillations in aged Dp(16)1Yey/+ mice: a down syndrome model, Neuroscience 376 (2018) 117–126. [PubMed: 29454635]

[24]. Davisson MT, Schmidt C, Akeson EC, Segmental trisomy of murine chromosome 16: a new model system for studying down syndrome, Prog. Clin. Biol. Res 360 (1990) 263–280. [PubMed: 2147289]

[25]. Li Z, Yu T, Morishima M, Pao A, LaDuca J, Conroy J, Nowak N, Matsui S, Shiraishi I, Yu YE, Duplication of the entire 22.9 Mb human chromosome 21 syntenic region on mouse chromosome 16 causes cardiovascular and gastrointestinal abnormalities, Hum. Mol. Genet 16 (11) (2007) 1359–1366. [PubMed: 17412756]

[26]. Goodliffe JW, Olmos-Serrano JL, Aziz NM, Pennings JL, Guedj F, Bianchi DW, Haydar TF, Absence of prenatal forebrain defects in the Dp(16)1Yey/+ mouse model of down syndrome, J. Neurosci 36 (10) (2016) 2926–2944. [PubMed: 26961948]

[27]. Blazek JD, Gaddy A, Meyer R, Roper RJ, Li J, Disruption of bone development and homeostasis by trisomy in Ts65Dn down syndrome mice, Bone 48 (2) (2011) 275–280. [PubMed: 20870049]

[28]. Fowler TW, McKelvey KD, Akel NS, Vander Schilden J, Bacon AW, Bracey JW, Sowder T, Skinner RA, Swain FL, Hogue WR, Leblanc DB, Gaddy D, Wenger GR, Suva LJ, Low bone turnover and low BMD in down syndrome: effect of intermittent PTH treatment, PLoS One 7 (8) (2012), e42967. [PubMed: 22916188]

[29]. Garcia Hoyos M, Humbert L, Salmon Z, Riancho JA, Valero C, Analysis of volumetric BMD in people with down syndrome using DXA-based 3D modeling, Arch. Osteoporos 14 (1) (2019) 98. [PubMed: 31494745]

[30]. Williams DK, Parham SG, Schryver E, Akel NS, Shelton RS, Webber J, Swain FL, Schmidt J, Suva LJ, Gaddy D, Sclerostin antibody treatment stimulates bone formation to normalize bone mass in male down syndrome mice, JBMR Plus 2 (1) (2018) 47–54. [PubMed: 30283889]

[31]. Bull MJ, Committee on G, Health supervision for children with Down syndrome, Pediatrics 128 (2) (2011) 393–406. [PubMed: 21788214]

[32]. Siris ES, Adler R, Bilezikian J, Bolognese M, Dawson-Hughes B, Favus MJ, Harris ST, Jan de Beur SM, Khosla S, Lane NE, Lindsay R, Nana AD, Orwoll ES, Saag K, Silverman S, Watts NB, The clinical diagnosis of osteoporosis: a position statement from the National Bone Health Alliance Working Group, Osteoporos. Int 25 (5) (2014) 1439–1443. [PubMed: 24577348]

[33]. Gonzalez-Aguero A, Vicente-Rodriguez G, Moreno LA, Casajus JA, Bone mass in male and female children and adolescents with Down syndrome, Osteoporos. Int 22 (7) (2011) 2151–2157. [PubMed: 20967423]

[34]. Kazuki Y, Gao FJ, Li Y, Moyer AJ, Devenney B, Hiramatsu K, Miyagawa-Tomita S, Abe S, Kazuki K, Kajitani N, Uno N, Takehara S, Takiguchi M, Yamakawa M, Hasegawa A, Shimizu R, Matsukura S, Noda N, Ogonuki N, Inoue K, Matoba S, Ogura A, Florea LD, Savonenko A, Xiao M, Wu D, Batista DA, Yang J, Qiu Z, Singh N, Richtsmeier JT, Takeuchi T, Oshimura M, Reeves RH, A non-mosaic transchromosomic mouse model of down syndrome carrying the long arm of human chromosome 21, elife 9 (2020).

[35]. Perrien DS, Akel NS, Edwards PK, Carver AA, Bendre MS, Swain FL, Skinner RA, Hogue WR, Nicks KM, Pierson TM, Suva LJ, Gaddy D, Inhibin a is an endocrine stimulator of bone mass and strength, Endocrinology 148 (4) (2007) 1654–1665. [PubMed: 17194739]

[36]. Suva LJ, Hartman E, Dilley JD, Russell S, Akel NS, Skinner RA, Hogue WR, Budde U, Varughese KI, Kanaji T, Ware J, Platelet dysfunction and a high bone mass phenotype in a murine model of platelet-type von willebrand disease, Am. J. Pathol 172 (2) (2008) 430–439. [PubMed: 18187573]

Author Manuscript Author Manuscript Author Manuscript Author Manuscript

[37]. Bouxsein ML, Boyd SK, Christiansen BA, Guldberg RE, Jepsen KJ, Muller R, Guidelines for assessment of bone microstructure in rodents using micro-computed tomography, J. Bone Miner. Res 25 (7) (2010) 1468–1486. [PubMed: 20533309]

[38]. Rzonca SO, Suva LJ, Gaddy D, Montague DC, Lecka-Czernik B, Bone is a target for the antidiabetic compound rosiglitazone, Endocrinology 145 (1) (2004) 401–406. [PubMed: 14500573]

[39]. Dempster DW, Compston JE, Drezner MK, Glorieux FH, Kanis JA, Malluche H, Meunier PJ, Ott SM, Recker RR, Parfitt AM, Standardized nomenclature, symbols, and units for bone histomorphometry: a 2012 update of the report of the ASBMR histomorphometry nomenclature committee, J. Bone Miner. Res 28 (1) (2013) 2–17. [PubMed: 23197339]

[40]. Dawson LA, Brunauer R, Zimmel KN, Qureshi O, Falck AR, Kim P, Dolan CP, Yu L, Lin YL, Daniel B, Yan M, Muneoka K, Adult mouse digit amputation and regeneration: a simple model to investigate mammalian blastema formation and intramembranous ossification, J. Vis. Exp 149 (2019).

[41]. Gaddy-Kurten D, Coker JK, Abe E, Jilka RL, Manolagas SC, Inhibin suppresses and activin stimulates osteoblastogenesis and osteoclastogenesis in murine bone marrow cultures, Endocrinology 143 (1) (2002) 74–83. [PubMed: 11751595]

[42]. Dawson LA, Schanes PP, Kim P, Imholt FM, Qureshi O, Dolan CP, Yu L, Yan M, Zimmel KN, Falck AR, Muneoka K, Blastema formation and periosteal ossification in the regenerating adult mouse digit, Wound Repair Regen. 26 (3) (2018) 263–273. [PubMed: 30120800]

[43]. Dolan CP, Dawson LA, Muneoka K, Digit tip regeneration: merging regeneration biology with regenerative medicine, Stem Cells Transl. Med 7 (3) (2018) 262–270. [PubMed: 29405625]

[44]. Simkin J, Sammarco MC, Dawson LA, Schanes PP, Yu L, Muneoka K, The mammalian blastema: regeneration at our fingertips, Regeneration (Oxf) 2 (3) (2015) 93–105. [PubMed: 27499871]

[45]. Dawson LA, Simkin J, Sauque M, Pela M, Palkowski T, Muneoka K, Analogous cellular contribution and healing mechanisms following digit amputation and phalangeal fracture in mice, Regeneration (Oxf) 3 (1) (2016) 39–51. [PubMed: 27499878]

[46]. Tamplen M, Fowler T, Markey J, Knott PD, Suva LJ, Alliston T, Treatment with anti-sclerostin antibody to stimulate mandibular bone formation, Head Neck 40 (7) (2018) 1453–1460. [PubMed: 29522281]

[47]. Stefanidis K, Belitsos P, Fotinos A, Makris N, Loutradis D, Antsaklis A, Causes of infertility in men with down syndrome, Andrologia 43 (5) (2011) 353–357. [PubMed: 21806650]

[48]. Blazek JD, Malik AM, Tischbein M, Arbones ML, Moore CS, Roper RJ, Abnormal mineralization of the Ts65Dn down syndrome mouse appendicular skeleton begins during embryonic development in a Dyrk1a-independent manner, Mech. Dev 136 (2015) 133–142. [PubMed: 25556111]

[49]. Thomas JR, LaCombe J, Long R, Lana-Elola E, Watson-Scales S, Wallace JM, Fisher EMC, Tybulewicz VLJ, Roper RJ, Interaction of sexual dimorphism and gene dosage imbalance in skeletal deficits associated with down syndrome, Bone 136 (2020), 115367. [PubMed: 32305495]

[50]. Whelan DB, Bhandari M, Stephen D, Kreder H, McKee MD, Zdero R, Schemitsch EH, Development of the radiographic union score for tibial fractures for the assessment of tibial fracture healing after intramedullary fixation, J. Trauma 68 (3) (2010) 629–632. [PubMed: 19996801]

[51]. Knox AM, McGuire AC, Natoli RM, Kacena MA, Collier CD, Methodology, selection, and integration of fracture healing assessments in mice, J. Orthop. Res 39 (11) (2021) 2295–2309. [PubMed: 34436797]

[52]. Suva LJ, Westhusin ME, Long CR, Gaddy D, Engineering bone phenotypes in domestic animals: unique resources for enhancing musculoskeletal research, Bone 130 (2020), 115119. [PubMed: 31712131]

[53]. Blazek JD, Abeysekera I, Li J, Roper RJ, Rescue of the abnormal skeletal phenotype in Ts65Dn down syndrome mice using genetic and therapeutic modulation of trisomic Dyrk1a, Hum. Mol. Genet 24 (20) (2015) 5687–5696. [PubMed: 26206885]

Author Manuscript Author Manuscript Author Manuscript Author Manuscript

[54]. Shaw PR, Klein JA, Aziz NM, Haydar TF, Longitudinal neuroanatomical and behavioral analyses show phenotypic drift and variability in the Ts65Dn mouse model of down syndrome, Dis. Model. Mech 13 (9) (2020).

[55]. Collaborative Cross C, The genome architecture of the Collaborative Cross mouse genetic reference population, Genetics 190 (2) (2012) 389–401. [PubMed: 22345608]

[56]. Hitzemann R, Phillips TJ, Lockwood DR, Darakjian P, Searles RP, Phenotypic and gene expression features associated with variation in chronic ethanol consumption in heterogeneous stock collaborative cross mice, Genomics 112 (6) (2020) 4516–4524. [PubMed: 32771621]

[57]. Eldridge R, Osorio D, Amstalden K, Edwards C, Young CR, Cai JJ, Konganti K, Hillhouse A, Threadgill DW, Welsh CJ, Brinkmeyer-Langford C, Antecedent presentation of neurological phenotypes in the collaborative cross reveals four classes with complex sex-dependencies, Sci. Rep 10 (1) (2020) 7918. [PubMed: 32404926]

[58]. Angelopoulou N, Matziari C, Tsimaras V, Sakadamis A, Souftas V, Mandroukas K, Bone mineral density and muscle strength in young men with mental retardation (with and without down syndrome), Calcif. Tissue Int 66 (3) (2000) 176–180. [PubMed: 10666490]

[59]. Baptista F, Varela A, Sardinha LB, Bone mineral mass in males and females with and without down syndrome, Osteoporos. Int 16 (4) (2005) 380–388. [PubMed: 15365695]

[60]. Carfi A, Liperoti R, Fusco D, Giovannini S, Brandi V, Vetrano DL, Meloni E, Mascia D, Villani ER, Manes Gravina E, Bernabei R, Onder G, Bone mineral density in adults with down syndrome, Osteoporos. Int 28 (10) (2017) 2929–2934. [PubMed: 28685282]

[61]. Costa R, De Miguel R, Garcia C, de Asua DR, Castaneda S, Moldenhauer F, Suarez C, Bone mass assessment in a cohort of adults with down syndrome: a cross-sectional study, Intellect. Dev. Disabil 55 (5) (2017) 315–324. [PubMed: 28972872]

[62]. Costa R, Gullon A, De Miguel R, de Asua DR, Bautista A, Garcia C, Suarez C, Castaneda S, Moldenhauer F, Bone mineral density distribution curves in spanish adults with down syndrome, J. Clin. Densitom 21 (4) (2018) 493–500. [PubMed: 29681439]

[63]. Deitz SL, Roper RJ, Trisomic and allelic differences influence phenotypic variability during development of down syndrome mice, Genetics 189 (4) (2011) 1487–1495. [PubMed: 21926299]

[64]. Gunderson ZJ, Campbell ZR, McKinley TO, Natoli RM, Kacena MA, A comprehensive review of mouse diaphyseal femur fracture models, Injury 51 (7) (2020) 1439–1447. [PubMed: 32362447]

[65]. Buettmann EG, McKenzie JA, Migotsky N, Sykes DA, Hu P, Yoneda S, Silva MJ, VEGFA from early osteoblast lineage cells (Osterix+) is required in mice for fracture healing, J. Bone Miner. Res 34 (9) (2019) 1690–1706. [PubMed: 31081125]

[66]. Litrenta J, Tornetta P 3rd, Mehta S, Jones C, O'Toole RV, Bhandari M, Kottmeier S, Ostrum R, Egol K, Ricci W, Schemitsch E, Horwitz D, Determination of radiographic healing: an assessment of consistency using RUST and modified RUST in metadiaphyseal fractures, J. Orthop. Trauma 29 (11) (2015) 516–520. [PubMed: 26165265]

[67]. Cooke ME, Hussein AI, Lybrand KE, Wulff A, Simmons E, Choi JH, Litrenta J, Ricci WM, Nascone JW, O'Toole RV, Morgan EF, Gerstenfeld LC, Tornetta P 3rd, Correlation between RUST assessments of fracture healing to structural and biomechanical properties, J. Orthop. Res 36 (3) (2018) 945–953. [PubMed: 28833572]

[68]. Tannenbaum TN, Lipworth L, Baker S, Risk of fractures in an intermediate care facility for persons with mental retardation, Am. J. Ment. Retard 93 (4) (1989) 444–451. [PubMed: 2930660]

[69]. van Allen MI, Fung J, Jurenka SB, Health care concerns and guidelines for adults with down syndrome, Am. J. Med. Genet 89 (2) (1999) 100–110. [PubMed: 10559765]

Author Manuscript Author Manuscript Author Manuscript Author Manuscript

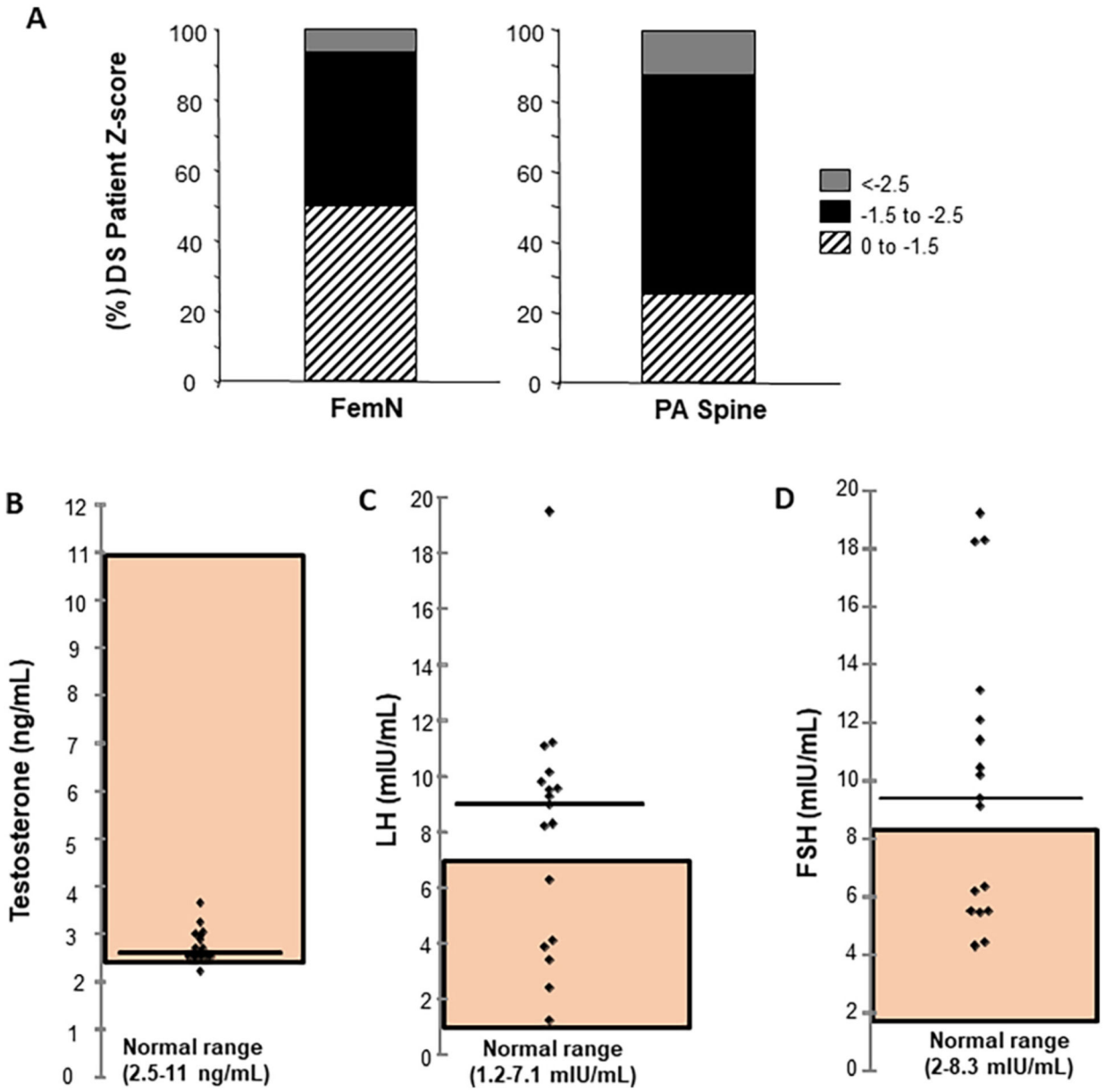

Fig. 1.

DS patient clinical parameters. (A) Distribution of male DS Bone Mineral Density (BMD) *Z*-scores at femoral neck (FemN) and posterior-anterior (PA) spine. Z score ranges 0 to −1.5; −1.5 to −2.5; and < −2.5 are indicated by hashed lines; black; gray shading respectively. The percentage of patients in each range is plotted ($n = 17$) (B) Serum measurements of individual testosterone (ng/ml) (C) Luteinizing hormone (LH) (mIU/ml), (D) Follicle stimulating hormone (FSH) (mIU/ml) levels in male DS patients. Normal range for each hormone indicated by shading. Horizontal line shows median hormone level for each measurement.

Author Manuscript
Author Manuscript
Author Manuscript
Author Manuscript

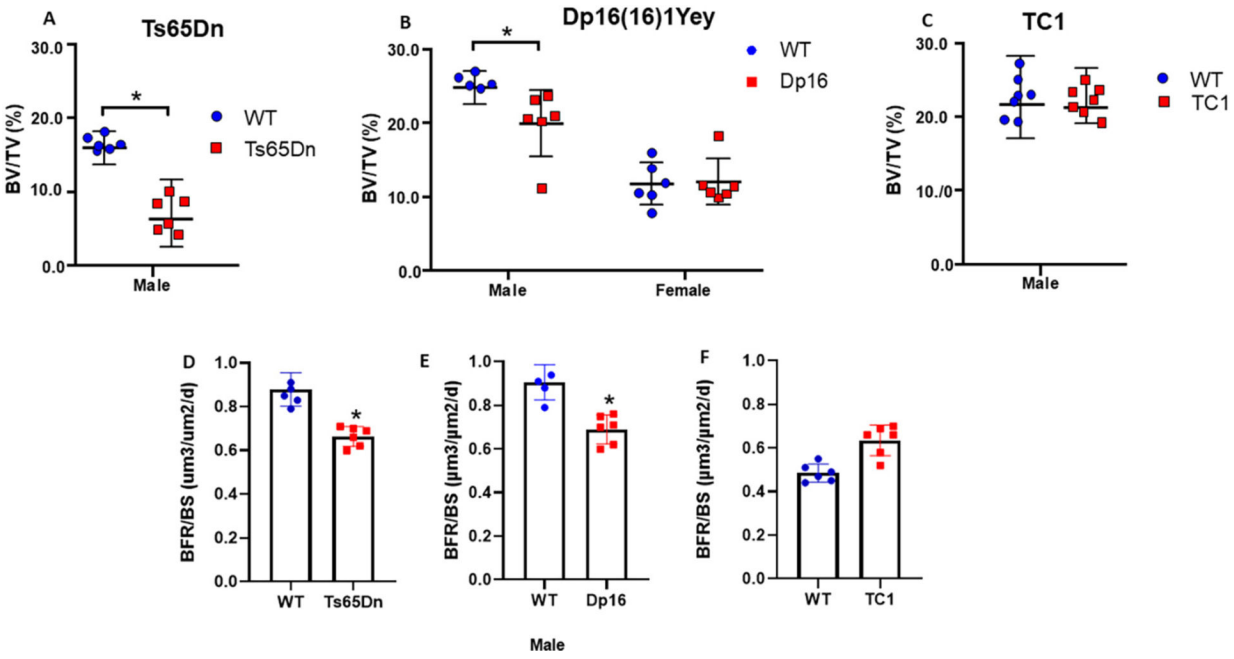

Fig. 2.

Bone volume and bone formation measurements in DS mouse tibiae. (A, D) BV/TV and bone formation rate per bone surface (BFR/BS) in male Ts65Dn; (B) BV/TV in male and female Dp16 DS mice and (E) bone formation rate per bone surface (BFR/BS) in male Dp16 DS mice. (C, F) BV/TV and bone formation rate per bone surface (BFR/BS) in male TC1 DS mice. *$p < 0.05$ between genotypes. MicroCT measurements shown for each individual animal; BFR/BS measured from fluorochrome labeling and dynamic histomorphometry from each animal, and calculated according to Dempster [39].

Author Manuscript Author Manuscript Author Manuscript Author Manuscript

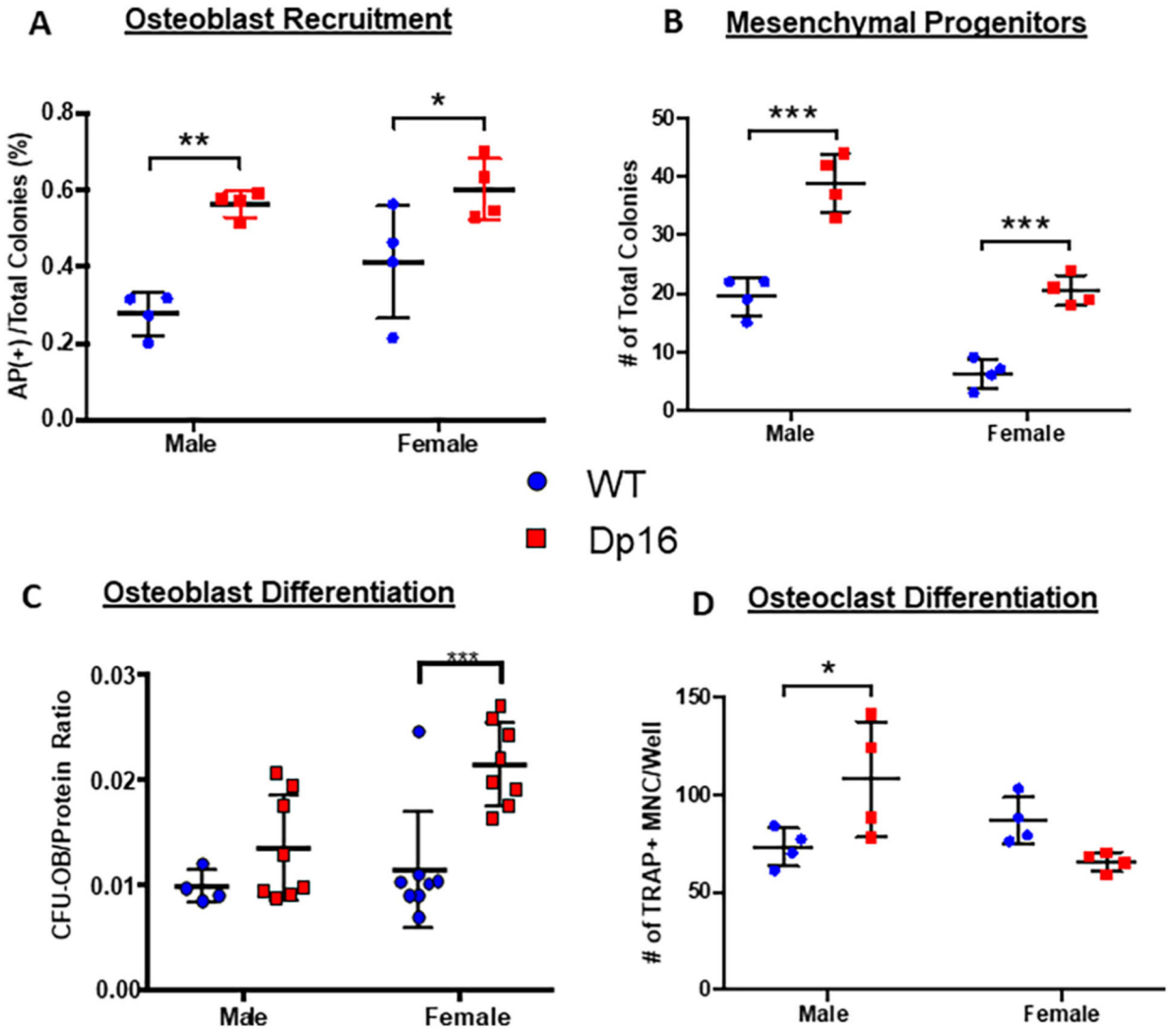

Fig. 3.

Dp16 DS *ex vivo* bone marrow cell differentiation. (A-C) Murine bone marrow cells from adult (3–4 months) WT (circles) and Dp16 DS (squares) male and female mice were cultured towards osteoblastogenesis. (A) Recruitment of cells into the osteoblast lineage was measured on d 10. The number of colonies staining positive for alkaline phosphatase (AP+) were counted and expressed as a percentage of the total number of colonies per well. (B) The total number of mesenchymal progenitors was determined in d 10 AP-stained and Fast green counter-stained dishes and both the number of AP+ colonies and the Fast green non-AP-stained colonies combined to express as total colonies per well. Number of mesenchymal progenitors was increased in both male and female Dp16 mice. (C) Mineralized osteoblastic colony-forming units (CFU-OB) were determined on d 28 by alizarin red staining, and the number of CFUOB normalized to the micrograms of protein content in each well. A significant increase in osteoblast differentiation capacity was observed in female Dp16 mice, but not male Dp16 mice. Data are representative of at least two similar experiments. $p < 0.05$ (*), $p < 0.002$ (**), or $p < 0.001$ (***) compared

Author Manuscript Author Manuscript Author Manuscript Author Manuscript

to WT gender-matched control. (D) Primary murine bone marrow cells were cultured for the development of osteoclasts. Cells were stained for TRAP activity, and the number of TRAP+ multinucleated cells (MNC) with 3 or more nuclei per well was counted. Data are representative of at least two similar experiments harvested on d 8–12. *$p < 0.05$.

Author Manuscript Author Manuscript Author Manuscript Author Manuscript

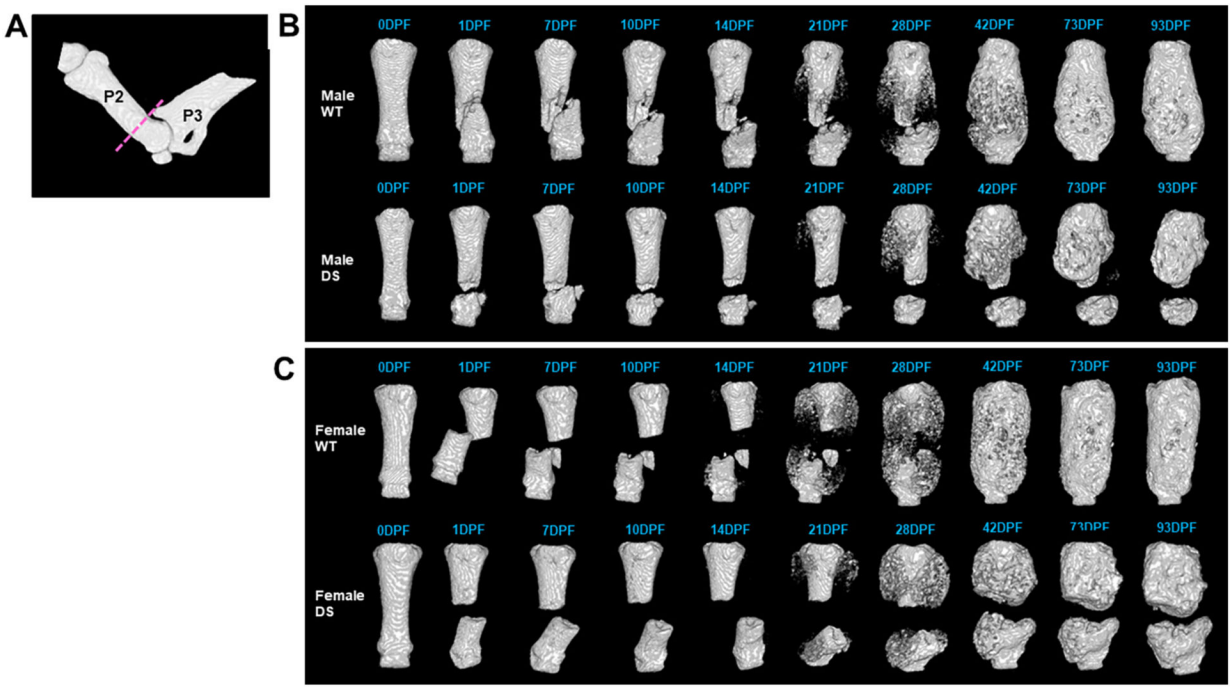

Fig. 4.

Time course of P2 Fracture Healing by *in vivo* microCT in WT and Dp16 DS mice. (A) MicroCT reconstruction of an intact P2 with the fracture plane (dashed line). *In vivo* microCT reconstructions of representative (B) male and (C) female WT and DS digits across the time course of fracture healing up to 93 days post-fracture (DPF). Normal fracture healing occurred in WT, with mineralization of the soft callus visible by 21 DPF, and fracture bridging by 42 DPF, when remodeling begins. Both male and female DS digits began mineralization by 21 DPF but did not successfully bridge by 42 DPF when WT digits were completely bridged and resulting in non-union fractures by 93 DPF.

Author Manuscript Author Manuscript Author Manuscript Author Manuscript

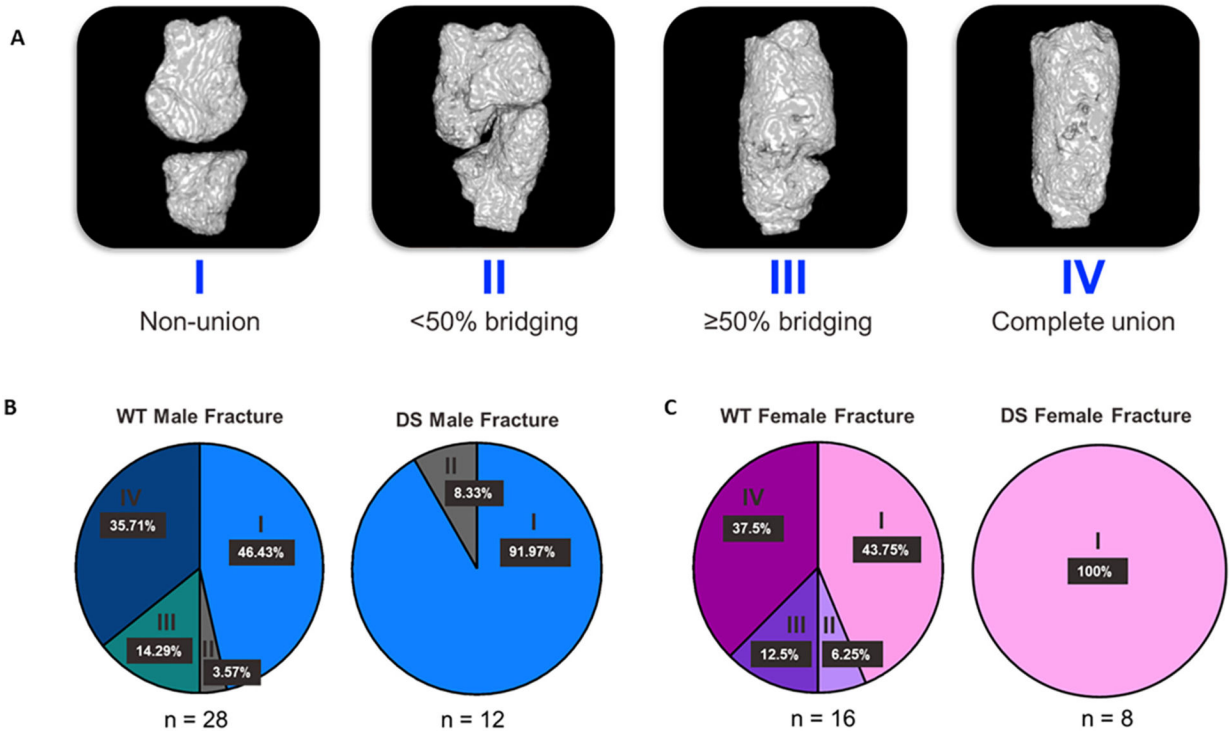

Fig. 5.

Computed Radiographic Assessment of P2 (CRAPP) Method for Fracture Scoring of Dp16 DS P2 Fractures. (A) *In vivo* microCT reconstructions of murine P2 digits demonstrating the use of CRAPP to quantify fracture healing. Fractures were scored from a range of I-IV, with I representing a non-union and IV representing a complete union, or healed fracture. Any fracture observed between two scores was assigned the lower score. (B) Fractures were scored using the CRAPP method, demonstrating a normal range of healing in both male and female WT mice. None of the DS fractures healed (score of IV), and most did not surpass a score of I in both males and females.

Author Manuscript
Author Manuscript
Author Manuscript
Author Manuscript

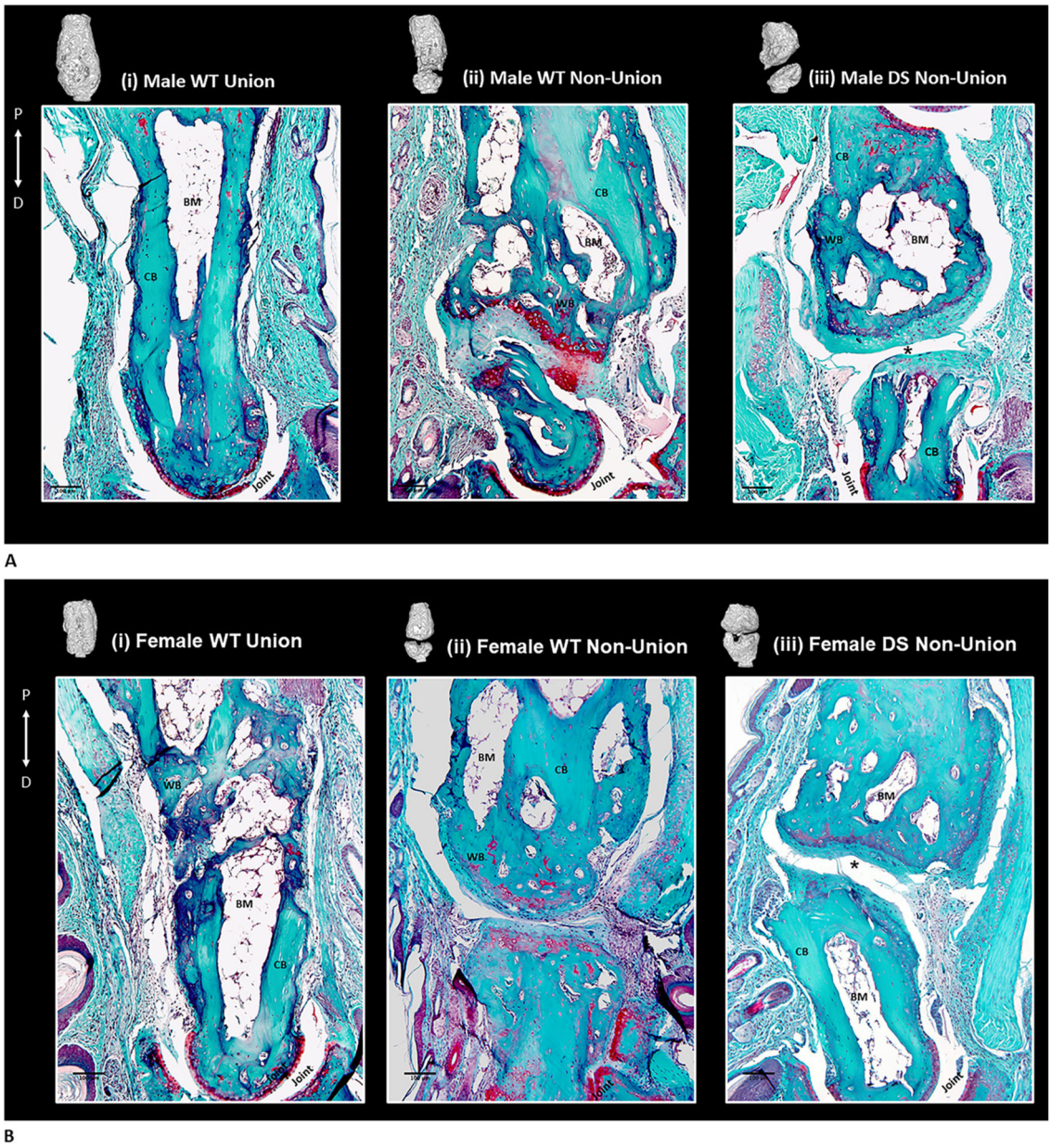

Fig. 6.

A: Male P2 fracture histology at 93 DPF. Safranin-O/Fast Green staining of male WT (i, ii) and Dp16 DS (iii) digits and the corresponding microCT reconstruction at 93DPF. Orientation is proximal (P) to distal (D). Bone is shown in green and cartilage proteoglycan is shown in red. (i) Bridged WT fracture, original fracture plane is not visible and the bony callus has been remodeled to lamellar cortical bone (CB) with a bone marrow (BM) cavity. (ii) WT non-union fracture shows extensive cortical bone (CB) proximal to the fracture gap, as well as intense red unmineralized cartilaginous proteoglycan-rich matrix surrounding chondrocytes in the fracture gap. (iii) DS non-union at 93DPF showing robust periosteal woven bone (WB) formation proximal to the fracture gap and the absence of red cartilaginous proteoglycan staining in the evident fracture gap (*). Scale bar is 100 μm.

Author Manuscript Author Manuscript Author Manuscript Author Manuscript

B: Female P2 fracture histology at 93 DPF.

Safranin-O/Fast Green staining of female WT (i, ii) and Dp16 DS (iii) digits and the corresponding microCT reconstruction at 93DPF. Orientation is proximal (P) to distal (D). Bone is shown in green and cartilage proteoglycan is shown in red. (i) Bridged WT female fracture, original fracture plane is not visible and the bony callus has been remodeled to lamellar cortical bone (CB) with a bone marrow (BM) cavity. (ii) WT female non-union fracture shows extensive cortical bone (CB) proximal to the fracture gap, as well as intense red unmineralized cartilaginous proteoglycan-rich matrix surrounding chondrocytes in the fracture gap. (iii) Female DS non-union at 93DPF showing robust periosteal woven bone (WB) formation proximal to the fracture gap and the absence of red cartilaginous proteoglycan staining in the evident fracture gap (*). Scale bar is 100um.